A Two-Dimensional Model of Hypertension-Induced Arterial Remodeling With Account for Stress Interaction Between Elastin and Collagen

Alexander Rachev[1]
University of South Carolina,
College of Engineering and Computing,
Biomedical Engineering Program,
Columbia, SC 29208;
Institute of Mechanics,
Acad. G Bonchev Street Block 4,
Sofia, Bulgaria
e-mail: a.i.rachev@gmail.com

Tarek Shazly
University of South Carolina,
College of Engineering and Computing,
Biomedical Engineering Program,
Columbia, SC 29208
e-mail: shazly@mailbox.sc.edu

We propose a novel structure-based two-dimensional (2D) mathematical model of hypertension-induced arterial remodeling. The model is built in the framework of the constrained mixture theory and global growth approach, utilizing a recently proposed structure-based constitutive model of arterial tissue that accounts for the individual natural configurations of and stress interaction between elastin and collagen. The basic novel predictive result is that provided remodeling causes a change in the elastin/collagen mass fraction ratio, it leads to a structural reorganization of collagen that manifests as an altered fiber undulation and a change in direction of the helically oriented fibers in the tissue natural state. Results obtained from the illustrative simulations for a porcine renal artery show that when remodeling is complete the collagen reorganization might have significant effects on the initial arterial geometry and mechanical properties of the arterial tissue. The proposed model has potential to describe and advance mechanistic understanding of adaptive arterial remodeling, promote the continual refinement of mathematical models of arterial remodeling, and provide motivation for new avenues of experimental investigation. [DOI: 10.1115/1.4045116]

Keywords: adaptive remodeling, structure-based constitutive modeling, constrained mixture theory, global growth approach

1 Introduction

Hypertension, defined as a persistent elevation of arterial pressure, is one of the major risk factors associated with the development of many diseases including heart attack, stroke, and kidney failure. Hypertension is recognized as a leading cause of morbidity and mortality in the western world. Arteries respond to long-term alterations in arterial pressure by changing geometry, structure, and composition. This response is termed remodeling and plays an important role in normal arterial physiology and in the genesis and progression of a wide range of vascular disorders. For example, an increase in arterial wall thickness and stiffness commonly occur at an early stage in the development of atherosclerosis (cf., Ref. [1]).

Remodeling results from the altered vascular cell activity caused by perturbed local stresses and strains, which trigger a series of events that may include cell proliferation, hyperplasia, apoptosis or necrosis, hypertrophy and migration, and may elicit an imbalance between extracellular matrix synthesis and degradation [2]. It has been experimentally established that in healthy mature arteries, remodeling results in restoration of the flow-induced shear stress at the endothelium and mean circumferential wall stress to certain baseline levels [2]. Therefore, in these cases, remodeling represents an adaptive process, which seeks to maintain the local mechanical environment of endothelial and smooth muscle cells (SMCs) despite changes in the global load conditions, and thereby preserves the optimal arterial performance. A comprehensive review of experimental investigations on adaptation and remodeling of arteries in response to hypertension is given in Ref. [3].

While experimental studies reveal important descriptive information, mathematical models offer a useful tool for testing plausible mechanisms of remodeling, obtaining predictive results, interpreting experimental data, and performing parametric studies for quantification of the effects of different factors involved in the remodeling process. Different theoretical approaches have been proposed to build mathematical models of adaptive hypertension-induced remodeling. Simultaneously and independently, the first theoretical studies on adaptive remodeling appeared in 1996 [4,5]. In Ref. [4], the authors adopted the volumetric growth approach considering the vessel as a collection of infinitesimal growing elements, which change their mass because of local stress or strain deviations from certain preferred baseline values according to postulated rate equations. In Ref. [5], the authors proposed a global growth approach considering the time variation of dimensions of an artery in the zero-stress state (ZSS) to be driven by the deviation of circumferential wall stress and flow-induced shear stress at the endothelium from certain homeostatic values via postulated evolution equations. Both the models used phenomenological constitutive formulations of arterial tissue and assumed that remodeling results solely in a change of arterial geometry while preserving mechanical properties of the tissue. To account for more specifics in the remodeling response, later models based on the volumetric growth approach were refined to introduce more realistic growth laws [6], consider an artery as a thick-walled or two-layered tube composed of a constrained mixture of SMCs, elastin, and collagen [6,7], include damage and plasticity [8], and capture changes in wall composition and mechanical homogeneity [9]. Similarly, models based on the global growth approach were refined to account for a change in mechanical properties by imposing a condition for restoration of arterial stiffness [10,11], consider the evolution of smooth muscle tone [12], and explain the spatial variation of hyperplasia at the artery/graft anastomosis [13]. A common characteristic among models based

[1]Corresponding author.

Manuscript received June 28, 2019; final manuscript received September 24, 2019; published online December 12, 2019. Assoc. Editor: Seungik Baek.

on volumetric or global growth is their focus on the kinematic consequences of remodeling rather than on the remodeling process itself. Recent models predict that properties of the tissue may change due to hypertension via a change in wall composition, but the individual mechanical properties of constituents remain unaffected by remodeling [4–9,12,13].

Inspired by the seminal paper [14], a new, fundamentally different approach to modeling arterial adaptation in hypertension based on description of biological events inherent to the remodeling process was proposed. Using the theory of constrained mixtures, a series of papers consider remodeling of the individual structural constituents that can have different natural configurations and can turnover at different rates, which implies interaction between the structurally significant constituents. The first one-layered two-dimensional (2D) model of this kind [15] was later refined to a three-dimensional approach [16], extended to a multilayered wall [17], and adapted to account for the effects of altered smooth muscle contractility and matrix growth [18]. It was shown that models can capture changes in arterial tissue composition and individual properties of the constituents in terms of the variable mass fractions and deposition stretches at which new mass is added and incorporated into existing tissue [19]. Though the deposition stretches and their rate of variation cannot be directly measured, a nonlinear regression approach was developed for identification of key model parameters from available histological and biaxial mechanical data [20]. Moreover, recent studies address directly the potential mediating role of inflammation in maladaptive arterial remodeling in hypertension [20,21] and found that mechanical properties are altered differentially in the media and adventitia [22,23].

In general, most of the proposed models focus on the time course of arterial remodeling following sustained elevation of arterial pressure by solving appropriate initial boundary value problems (e.g., Refs. [4–9]) or using hereditary integral formulations, (e.g., Refs. [19,24], and [25]) after a stepwise change in arterial pressure. A few models address the direct determination of the final remodeled state of the arterial wall by seeking the stationary solution of a system of transcendental equations that describe the deformation process and the conditions reflecting the adaptive nature of remodeling (e.g., Refs. [26] and [27]). Recently, the critical role of the relative rates of tissue responses and external loading was examined and a new rate-independent approach for modeling the evolution of soft tissue growth and remodeling was proposed [28].

To our knowledge, none of the published models predict how the stress interaction between elastin and collagen is modulated by remodeling in hypertension and affects remodeling outputs. The aim of this study is to propose a predictive 2D model for the final effects of adaptive remodeling in hypertension of healthy arteries. It accounts explicitly for the stress interaction between elastin and collagen which affects arterial geometry and can cause a structural reorganization of the collagen network. The model is built in the framework of the global growth approach, utilizing a recently proposed structure-based constitutive model of arterial tissue [29].

2 Mathematical Model

A healthy, mature artery under normal load conditions and after reaching stationary state as a result of adaptive remodeling induced by a sustained increase in pressure is termed as normotensive and hypertensive, respectively. First, we consider the stretch and stress field of the normotensive artery. Later, using the global growth approach, we determine the ZSS geometry, arterial wall composition, structural organization of collagen network, and mechanical response of the hypertensive artery when adaptive pressure-induced remodeling is completed.

2.1 Normotensive Artery. Following the 2D approach [30,31], an artery is considered as a membrane made of an elastic incompressible material. In the stress-free configuration, κ_0^N (Fig. 1), the inner radius is R_i^N and thickness H^N. Hereafter, the superscript N denotes quantities in the normotensive artery. Under internal pressure P^N and longitudinal in situ stretch λ^N, the artery undergoes a finite axisymmetric deformation and takes the deformed configuration κ^N (Fig. 1) with inner radius r_i^N and wall thickness h^N; $\lambda^N = L/L_0^N, L$ and L_0^N are the lengths of arterial segment in situ and in the traction-free state, respectively. Considering an artery as a membrane the traction-free state is also a ZSS. The deformation is described in terms of the circumferential and axial stretch of the arterial midwall surface with respect to a cylindrical coordinate system and by the change in wall thickness with account for the material incompressibility, as follows:

$$\lambda_\theta^N = \frac{r_i^N + h^N/2}{R_i^N + H^N/2}, \quad \lambda_z^N = \lambda^N, \qquad h^N = \frac{H^N}{\lambda_\theta^N \lambda_z^N} \tag{1}$$

Expressions for the mean stresses produced by deformation depend on the adopted constitutive model of arterial tissue. We use the 2D structure-based constitutive formulation given recently in Ref. [29]. Briefly, the tissue is considered as a constrained mixture of collagen and elastin each having an individual zero-stress (natural) configuration. Elastin is considered as an isotropic neo-Hookean solid. Collagen exists as four fiber families with dominant orientation as follows: a longitudinally oriented family (1); a circumferentially oriented family (2); and two helically oriented families (3) and (4) that are symmetrical with respect to the longitudinal direction. Each collagen family represents a collection of an infinite number of fiber subfamilies with identical orientation but continuously varying waviness in the state when the tissue is not stretched. In the tissue natural state elastin is biaxially extended while collagen fibers are compressed, and the partial stress borne by each constituent is self-equilibrated. When an artery is inflated and extended, depending on the fiber orientation, degree of initial undulation, and magnitude of circumferential and axial stretch, some fibers might be compressed, extended but not straightened, or straightened and stretched. The stress response of fibers under compression is described by a strain energy function (SEF) that is a sum of exponential functions of the tissue stretch along jth fiber direction family $(j = 1, \ldots 4)$. In line with the continuum-based approach, the mechanical properties of each collagen subfamily are described by a solid with SEF that is a quadratic function of the Green strain in the direction of fibers when

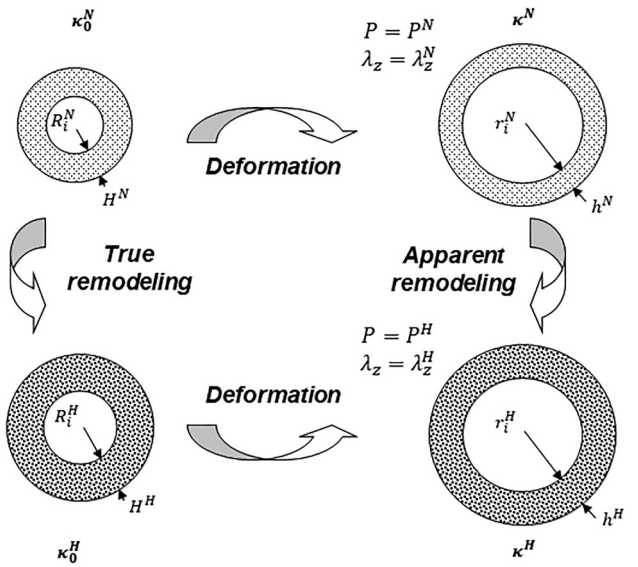

Fig. 1 Schematic of the arterial configurations before and after pressure-induced remodeling

they are straightened and stretched. According to the rule of mixtures, the total SEF and tissue stress produced by the constituents is a sum of the individual SEFs, or respectively, effective stress, of each load-bearing constituent weighted by its mass fraction as follows:

$$\begin{aligned}\sigma_\theta^N &= 2\varphi_{\mathrm{el}}^N \mathrm{c}_{\mathrm{el}}\left(\left(\lambda_{\mathrm{el}(\theta)}^0\lambda_\theta^N\right)^2-\frac{1}{\left(\lambda_{\mathrm{el}(\theta)}^0\lambda_\theta^N\right)^2\left(\lambda_{\mathrm{el}(z)}^0\lambda_z^N\right)^2}\right)\\&+\lambda_{\mathrm{col}(\theta)}^0\lambda_\theta^N\sum_{j=1}^4\gamma^{(j)N}\varphi_{\mathrm{col}}^{(j)N}\left\{\mathrm{c}_1^{(j)\mathrm{c}}\left(\left(\lambda_{\mathrm{col}}^{(j)N}\right)^2-1\right)\right.\\&\left.\times\exp\left[\mathrm{c}_2^{(j)\mathrm{c}}\left(\left(\lambda_{\mathrm{col}}^{(j)N}\right)^2-1\right)^2\right]\right\}\sin^2\beta_0^{(j)N}\\&+\sum_{j=1}^4\mathrm{c}_{\mathrm{col}}\Delta\lambda_r^{(j)N}\int_0^{\hat{\alpha}_{(i)}^{(j)N}}\varphi_{\mathrm{col}(i)}^{(j)N}E_{\mathrm{col}(i)}^{(j)N}\left(\frac{\lambda_\theta^N}{\lambda_{r(i)}^{(j)N}}\right)^2\sin^2\beta^{(j)N}d\alpha_{(i)}^{(j)N}\\\sigma_z^N &= 2\varphi_{\mathrm{el}}^N \mathrm{c}_{\mathrm{el}}\left(\left(\lambda_{\mathrm{el}(z)}^0\lambda_z^N\right)^2-\frac{1}{\left(\lambda_{\mathrm{el}(\theta)}^0\lambda_\theta^N\right)^2\left(\lambda_{\mathrm{el}(z)}^0\lambda_z^N\right)^2}\right)\\&+\lambda_{\mathrm{col}(z)}^0\lambda_z^N\sum_{j=1}^4\gamma^{(j)N}\varphi_{\mathrm{col}}^{(j)N}\left\{\mathrm{c}_1^{(j)\mathrm{c}}\left(\left(\lambda_{\mathrm{col}}^{(j)N}\right)^2-1\right)\right.\\&\left.\times\exp\left[\mathrm{c}_2^{(j)\mathrm{c}}\left(\left(\lambda_{\mathrm{col}}^{(j)N}\right)^2-1\right)^2\right]\right\}\cos^2\beta_0^{(j)N}\\&+\sum_{j=1}^4\mathrm{c}_{\mathrm{col}}\Delta\lambda_r^{(j)N}\int_0^{\hat{\alpha}_{(i)}^{(j)N}}\varphi_{\mathrm{col}(i)}^{(j)N}E_{\mathrm{col}(i)}^{(j)N}\left(\frac{\lambda_z^N}{\lambda_{r(i)}^{(j)N}}\right)^2\cos^2\beta^{(j)N}d\alpha_{(i)}^{(j)N}\end{aligned}\tag{2}$$

where

$$\hat{\alpha}_{(i)}^{(j)N}=\begin{cases}0 & \text{if } \lambda^{(j)N}<\lambda_{r(\min)}^{(j)N}\\ \dfrac{\lambda^{(j)N}-\lambda_{r(\min)}^{(j)N}}{\Delta\lambda_r^{(j)N}} & \text{if } \lambda_{r(\min)}^{(j)N}<\lambda^{(j)N}<\lambda_{r(\max)}^{(j)N}\\ 1 & \text{if } \lambda^{(j)N}>\lambda_{r(\max)}^{(j)N}\end{cases}\tag{3}$$

$$\gamma^{(j)N}=\begin{cases}1 & \text{if } \lambda_{\mathrm{col}}^{(j)N}<1\\ 0 & \text{if } \lambda_{\mathrm{col}}^{(j)N}\geq 1\end{cases}$$

$\lambda_{\mathrm{el}(\theta)}^0>1$, $\lambda_{\mathrm{el}(z)}^0>1$, $\lambda_{\mathrm{col}(\theta)}^0<1$, and $\lambda_{\mathrm{col}(z)}^0<1$ are the initial prestretches of elastin and collagen in the tissue ZSS in the circumferential and axial directions, respectively; $\beta_0^{(j)N}$ is the angle with respect to the longitudinal direction of the jth family collagen fibers in the natural configuration of collagen, which is calculated from the relation $\beta^{(j)N}=\arccos\left[\cos\beta_0^{(j)N}\lambda_{\mathrm{col}(z)}^0/\lambda_{\mathrm{col}}^{0(j)N}\right]$, where $\beta^{(j)N}$ is the corresponding angle of the jth family collagen fibers in the natural configuration of the tissue, which can be determined from histology, and $\lambda_{\mathrm{col}}^{0(j)N}=\sqrt{(\lambda_{\mathrm{col}(\theta)}^0)^2\sin^2\beta_0^{(j)N}+(\lambda_{\mathrm{col}(z)}^0)^2\cos^2\beta_0^{(j)N}}$ is the prestretch experienced by a linear element oriented along the jth family of the collagen in the normotensive artery natural state; $\lambda_{\mathrm{col}}^{(j)N}=\sqrt{(\lambda_{\mathrm{col}(\theta)}^0\lambda_\theta^N)^2\sin^2\beta_0^{(j)N}+(\lambda_{\mathrm{col}(z)}^0\lambda_z^N)^2\cos^2\beta_0^{(j)N}}$ and $\lambda^{(j)N}=\sqrt{(\lambda_\theta^N)^2\sin^2\beta^{(j)N}+(\lambda_z^N)^2\cos^2\beta^{(j)N}}$ are the stretches along the jth family of the collagen in the deformed tissue state with respect to collagen and tissue natural state, respectively; $\lambda_{\mathrm{col}(i)}^{(j)N}=\lambda^{(j)N}/\lambda_{r(i)}^{(j)N}$ and $E_{\mathrm{col}(i)}^{(j)N}=\frac{1}{2}\left((\lambda_{\mathrm{col}(i)}^{(j)N})^2-1\right)$ are the stretch and the corresponding Green strain experienced along the collagen fibers when they are straightened and stretched, where $\lambda_{r(i)}^{(j)N}=\lambda_{r(\min)}^{(j)N}+\alpha_{(i)}^{(j)N}\Delta\lambda_r^{(j)N}$ is the so-called recruitment stretch defined with respect to the tissue natural state that is needed to straighten ith subfamily fibers of the jth family [29] and has to be determined from histology as explained in Ref. [32]; $\lambda_{r(\min)}^{(j)N}$ and $\lambda_{r(\max)}^{(j)N}$ are the recruitment stretches corresponding to the least and most undulated jth family fibers, respectively; $\Delta\lambda_r^{(j)N}=\lambda_{r(\max)}^{(j)N}-\lambda_{r(\min)}^{(j)N}$; $\alpha_{(i)}^{(j)N}$ is a dimensionless parameter that varies over the interval $[0, 1]$; φ_{el}^N and $\varphi_{\mathrm{col}}^{(j)N}$ are the mass fractions of elastin and the jth collagen fiber family, defined as a ratio between the constituent mass and total tissue mass in a unit volume; $\varphi_{\mathrm{col}(i)}^{(j)N}$ are the mass fraction intensity functions that describe the distribution of collagen mass fraction among fibers with identical orientation but different waviness; $\varphi_{\mathrm{col}(i)}^{(j)N}$ is a continuous function of the recruitment stretch $\lambda_{r(i)}^{(j)N}$ over the range $\left[\lambda_{r(\min)}^{(j)N},\lambda_{r(\max)}^{(j)N}\right]$. Given $\lambda_{r(\min)}^{(j)N}$ and $\lambda_{r(\max)}^{(j)N}$, $\varphi_{\mathrm{col}(i)}^{(j)N}$ can be considered also as a function of $\alpha_{(i)}^{(j)N}$. The experimental findings in Ref. [32] showed that range in variation of recruitment stretch does not depend on the fiber orientation. Therefore, parameters $\lambda_{r(\min)}^{(j)N}$ and $\lambda_{r(\max)}^{(j)N}$ for a normotensive artery are identical for each fiber family. Obviously, the following equation holds true:

$$\Delta\lambda_r^{(j)N}\int_0^1\varphi_{\mathrm{col}(i)}^{(j)N}d\alpha_{(i)}^{(j)N}=\varphi_{\mathrm{col}}^{(j)N}\tag{4}$$

Parameters $\hat{\alpha}_{(i)}^{(j)N}$ and $\gamma^{(j)N}$ govern the engagement of fibers in tension and compression, respectively. Finally, c_{el}, $\mathrm{c}_1^{(j)\mathrm{c}}$, $\mathrm{c}_2^{(j)\mathrm{c}}$, and $\mathrm{c}_{\mathrm{col}}$ are material constants of elastin, collagen in compression, and collagen in tension, respectively.

In the tissue natural state, $\lambda_\theta^N=\lambda_Z^N=1$ and the partial stresses borne by elastin and collagen are self-equilibrated and therefore

$$\begin{aligned}&2\varphi_{\mathrm{el}}^N\mathrm{c}_{\mathrm{el}}\left(\left(\lambda_{\mathrm{el}(\theta)}^0\right)^2-\frac{1}{\left(\lambda_{\mathrm{el}(\theta)}^0\right)^2\left(\lambda_{\mathrm{el}(z)}^0\right)^2}\right)\\&+\lambda_{\mathrm{col}(\theta)}^0\sum_{j=1}^4\varphi_{\mathrm{col}}^{(j)N}\left\{\mathrm{c}_1^{(j)\mathrm{c}}\left(\left(\lambda_{\mathrm{col}}^{0(j)N}\right)^2-1\right)\right.\\&\left.\times\exp\left[\mathrm{c}_2^{(j)\mathrm{c}}\left(\left(\lambda_{\mathrm{col}}^{0(j)N}\right)^2-1\right)^2\right]\right\}\sin^2\beta_0^{(j)N}=0\\&2\varphi_{\mathrm{el}}^N\mathrm{c}_{\mathrm{el}}\left(\left(\lambda_{\mathrm{el}(z)}^0\right)^2-\frac{1}{\left(\lambda_{\mathrm{el}(\theta)}^0\right)^2\left(\lambda_{\mathrm{el}(z)}^0\right)^2}\right)\\&+\lambda_{\mathrm{col}(z)}^0\sum_{j=1}^4\varphi_{\mathrm{col}}^{(j)N}\left\{\mathrm{c}_1^{(j)\mathrm{c}}\left(\left(\lambda_{\mathrm{col}}^{0(j)N}\right)^2-1\right)\right.\\&\left.\times\exp\left[\mathrm{c}_2^{(j)\mathrm{c}}\left(\left(\lambda_{\mathrm{col}}^{0(j)N}\right)^2-1\right)^2\right]\right\}\cos^2\beta_0^{(j)N}=0\end{aligned}\tag{5}$$

Equations (5) are fundamental for the constitutive model and express the coupling between elastin and collagen prestretches

that modulate the interaction between their individual stress responses.

Given the initial arterial geometry, structural and mechanical constitutive parameters, and axial stretch λ_z^N, the deformed and stress states of the artery are determined provided the circumferential tissue stretch λ_θ^N satisfies the equation of equilibrium that follows from the free-body diagram of the inflated artery, namely, $\sigma_\theta^N - P^N r_i^N / h^N = 0$, where σ_θ^N is given by the first of Eq. (2).

2.2 Hypertensive Artery. When the vessel is kept at constant length and arterial pressure increases in a stepwise manner to P^H, the artery undergoes an instantaneous elastic deformation and the inner diameter increases. Hereafter, the superscript H denotes quantities in the hypertensive artery. The elastic response is followed by an acute vasomotor response that tends to reduce the increased deformed diameter and thereby diminish the disturbing effects on the mechanosensitive vascular cells caused by the decreased flow-induced shear stress at the endothelium and increased mean circumferential stress in the arterial wall (cf., Refs. [9] and [31]). Persisting elevation of the arterial pressure triggers time-dependent remodeling of the artery that ultimately leads to the establishing of a new steady-state with resorted vascular homeostasis. In the final deformed configuration, κ^H (Fig. 1), remodeling manifests as a change in arterial dimensions and eventually composition and structural organization of the arterial wall. The deformed inner radius is r_i^H and wall thickness is h^H. When applied loads are removed the artery takes the stress-free configuration κ_0^H with inner radius R_i^H and thickness H^H. Similar to the case of normotensive artery, the deformation is described by the circumferential and axial stretches of the midwall surface and the change in wall thickness as follows:

$$\lambda_\theta^H = \frac{r_i^H + h^H/2}{R_i^H + H^H/2}, \quad \lambda_z^H, \quad h^H = \frac{H^H}{\lambda_\theta^H \lambda_z^H} \tag{6}$$

Due to remodeling the total mass of the hypertensive artery alters. Considering the case when the artery is kept at constant deformed length, the ratio between the total mass of hypertensive and normotensive artery is $K = \left(R_i^H + H^H/2\right)\lambda_z^N / \left(R_i^N + H^N/2\right)\lambda_z^H$. The new mass is distributed among elastin, collagen, and SMCs. The literature provides contradictory experimental data for the change in mass fractions of wall constituents due to remodeling [3]. We consider several typical scenarios for the effects of adaptive remodeling on tissue composition of hypertensive arteries.

Case 1. The mass of elastin is taken to be constant and the collagen mass fraction remains as it is in the normotensive artery. Recalling the definition of mass fractions as a ratio of the constituent mass and total arterial mass per unit volume and the condition that the sum of all mass fractions is equal to one, the relations which follow are:

$$\varphi_{\mathrm{el}}^H = \frac{1}{K}\varphi_{\mathrm{el}}^N, \quad \varphi_{\mathrm{col}}^{(j)H} = \varphi_{\mathrm{col}}^{(j)N}, \qquad \varphi_{\mathrm{sm}}^H = 1 - \varphi_{\mathrm{el}}^H - \sum_1^4 \varphi_{\mathrm{col}}^{(j)H} \tag{7}$$

Rationale for case 1 is the experimentally established fact that in a mature organism, the turnover of elastin and its age-related functional degradation are very slow processes with a characteristic time much bigger than the duration of remodeling [2]. Case 1 is supported also by experimental findings in Ref. [33] that in a common carotid artery of mature Wistar rats the mass fraction of elastin decreases while the mass fraction of collagen remains unchanged after deoxycorticosterone acetate (DOCA)-salt induced hypertension. A small change in collagen mass fraction in the rat aortic wall caused by hypertension was also reported in Refs. [34] and [35]. In this case, the mass of the hypertensive arteries increases mainly as a result of SMC hypertrophy and hyperplasia, as well as upregulated collagen synthesis that keeps its mass fraction constant.

Case 2. Both the mass fractions of elastin and collagen increase due to remodeling and the new collagen mass is distributed proportionally among fiber families such that

$$\varphi_{\mathrm{el}}^H = \omega_{\mathrm{el}}(P)\,\varphi_{\mathrm{el}}^N, \quad \varphi_{\mathrm{col}}^{(j)H} = \omega_{\mathrm{col}}(P)\varphi_{\mathrm{col}}^{(j)N}, \qquad \varphi_{\mathrm{sm}}^H = 1 - \omega_{\mathrm{el}}(P)\varphi_{\mathrm{el}}^N - \omega_{\mathrm{col}}(P)\sum_1^4 \varphi_{\mathrm{col}}^{(j)N} \tag{8}$$

Functions $\omega_{\mathrm{el}}(P) > 1$ and $\omega_{\mathrm{col}}(P) > 1$, such that $\omega_{\mathrm{el}}(P^N) = \omega_{\mathrm{col}}(P^N) = 1$, are to be determined from histology at different levels of hypertension. An increase in both the elastin and collagen mass fractions is documented in young rat's carotid in the experimental model of hypertension induced by ligation of the renal arteries [36].

Case 3. This is the trivial case when remodeling does not affect the composition of arterial tissue as observed in Ref. [37] and assumed in some published models (e.g., Refs. [4–6]). Therefore,

$$\varphi_{\mathrm{el}}^H = \varphi_{\mathrm{el}}^N, \qquad \varphi_{\mathrm{col}}^{(j)H} = \varphi_{\mathrm{col}}^{(j)N}, \qquad \varphi_{\mathrm{sm}}^H = 1 - \varphi_{\mathrm{el}}^H - \sum_1^4 \varphi_{\mathrm{col}}^{(j)H} \tag{9}$$

If the remodeling-induced change in arterial mass alters the elastin/collagen mass fraction ratio, Eqs. (5) for self-equilibration of partial stresses borne by elastin and collagen are no longer satisfied. To restore the equilibrium in the ZSS of the hypertensive artery, the prestretch of elastin and collagen must change accordingly. Because the arterial tissue is modeled as a constrained mixture, elastin and collagen experience identical additional "remodeling-induced" circumferential and axial prestretches $\lambda_{\mathrm{rem}(\theta)}$ and $\lambda_{\mathrm{rem}(z)}$ such that the following equations hold true:

$$\begin{aligned}
&2\varphi_{\mathrm{el}}^H \mathrm{c}_{\mathrm{el}}\left(\left(\lambda_{\mathrm{el}(\theta)}^0\lambda_{\mathrm{rem}(\theta)}\right)^2 - \frac{1}{\left(\lambda_{\mathrm{el}(\theta)}^0\lambda_{\mathrm{rem}(\theta)}\right)^2\left(\lambda_{\mathrm{el}(z)}^0\lambda_{\mathrm{rem}(z)}\right)^2}\right)\\
&\quad + \lambda_{\mathrm{col}(\theta)}^0\lambda_{\mathrm{rem}(\theta)}\sum_{j=1}^4 \varphi_{\mathrm{col}}^{(j)H}\left\{\mathrm{c}_1^{(j)\mathrm{c}}\left(\left(\lambda_{\mathrm{col}}^{0(j)H}\right)^2 - 1\right)\right.\\
&\quad \left.\times \exp\left[\mathrm{c}_2^{(j)\mathrm{c}}\left(\left(\lambda_{\mathrm{col}}^{0(j)H}\right)^2 - 1\right)^2\right]\right\}\sin^2\beta_0^{(j)N} = 0\\
&2\varphi_{\mathrm{el}}^H \mathrm{c}_{\mathrm{el}}\left(\left(\lambda_{\mathrm{el}(z)}^0\lambda_{\mathrm{rem}(z)}\right)^2 - \frac{1}{\left(\lambda_{\mathrm{el}(\theta)}^0\lambda_{\mathrm{rem}(\theta)}\right)^2\left(\lambda_{\mathrm{el}(z)}^0\lambda_{\mathrm{rem}(z)}\right)^2}\right)\\
&\quad + \lambda_{\mathrm{col}(z)}^0\lambda_{\mathrm{rem}(z)}\sum_{j=1}^4 \varphi_{\mathrm{col}}^{(j)H}\left\{\mathrm{c}_1^{(j)\mathrm{c}}\left(\left(\lambda_{\mathrm{col}}^{0(j)H}\right)^2 - 1\right)\right.\\
&\quad \left.\times \exp\left[\mathrm{c}_2^{(j)\mathrm{c}}\left(\left(\lambda_{\mathrm{col}}^{0(j)H}\right)^2 - 1\right)^2\right]\right\}\cos^2\beta_0^{(j)N} = 0
\end{aligned} \tag{10}$$

where $\lambda_{\mathrm{col}}^{0(j)H} = \lambda_{\mathrm{rem}}^{(j)}\lambda_{\mathrm{col}}^{0(j)N} = \sqrt{\left(\lambda_{\mathrm{col}(\theta)}^0\lambda_{\mathrm{rem}(\theta)}\right)^2\sin^2\beta_0^{(j)N} + \left(\lambda_{\mathrm{col}(z)}^0\lambda_{\mathrm{rem}(z)}\right)^2\cos^2\beta_0^{(j)N}}$ is the prestretch experienced the direction of jth family fibers of the hypertensive artery in its natural state and $\lambda_{\mathrm{rem}}^{(j)} = \sqrt{\lambda_{\mathrm{rem}(\theta)}^2\sin^2\beta^{(j)N} + \lambda_{\mathrm{rem}(z)}^2\cos^2\beta^{(j)N}}$ is the additional "remodeling-induced" stretch; $\beta^{(j)H} = \arccos\left[\cos\beta^{(j)N}\lambda_{\mathrm{rem}(z)}/\lambda_{\mathrm{rem}}^{(j)}\right]$ is the angle of jth family fibers in the natural state of the hypertensive artery, which differs from $\beta^{(j)N}$ only for helically oriented families.

Equations (10) are the keystone relations in the proposed model. They account for the remodeling-induced alteration in stress interaction between elastin and collagen via altered prestretches in the ZSS of the hypertensive artery. Obviously, in case 3, $\lambda_{\mathrm{rem}(\theta)} = \lambda_{\mathrm{rem}(z)} = 1$, and the hypertensive artery exhibits mechanical properties that are identical to the normotensive vessel.

The products $\lambda^0_{\mathrm{el}(\theta)}\lambda_{\mathrm{rem}(\theta)}$, $\lambda^0_{\mathrm{el}(z)}\lambda_{\mathrm{rem}(z)}$, $\lambda^0_{\mathrm{col}(\theta)}\lambda_{\mathrm{rem}(\theta)}$, and $\lambda^0_{\mathrm{col}(z)}\lambda_{\mathrm{rem}(z)}$ are the effective values of elastin and collagen prestretches in the natural state of the hypertensive artery. The modified collagen prestretch affects the structural organization of the collagen fibers. The collagen mass fraction intensity functions $\varphi^{(j)H}_{\mathrm{col}(i)}$ are defined over a new fiber family-specific recruitment stretch interval $[\lambda^{(j)H}_{r(\min)}, \lambda^{(j)H}_{r(\max)}]$, where $\lambda^{(j)H}_{r(\min)} = \lambda^{(j)N}_{r(\min)}/\lambda^{(j)}_{\mathrm{rem}}$, $\lambda^{(j)H}_{r(\max)} = \lambda^{(j)N}_{r(\max)}/\lambda^{(j)}_{\mathrm{rem}}$. This means that in contrast to the normotensive artery, the mass distribution for each collagen family of the hypertensive artery is family specific. Accounting for constant arterial length, the axial stretch becomes $\lambda^H_z = \lambda^N_z/\lambda_{\mathrm{rem(z)}}$.

Similar to the case of normotensive artery, the following equations hold true

$$\Delta\lambda^{(j)H}_r \int_0^1 \varphi^{(j)H}_{\mathrm{col}(i)} d\alpha^{(j)H}_{(i)} = \varphi^{(j)H}_{\mathrm{col}} \qquad (\mathrm{j} = 1,\ 2,\ \text{or } 4) \tag{11}$$

which allow introducing as unknown one, two, or three family specific model parameters, say $k^{(j)}_{\mathrm{col}}$, that describe effects of remodeling on mass fraction intensity functions $\varphi^{(j)H}_{\mathrm{col}(i)}$.

Finally, the circumferential and axial stress–stretch relations for the tissue of the hypertensive artery are

$$\begin{aligned}\sigma^H_\theta = {} & 2\varphi^H_{\mathrm{el}}\mathrm{c}_{\mathrm{el}}\left(\left(\lambda^0_{\mathrm{el}(\theta)}\lambda_{\mathrm{rem}(\theta)}\lambda^H_\theta\right)^2 - \frac{1}{\left(\lambda^0_{\mathrm{el}(\theta)}\lambda_{\mathrm{rem}(\theta)}\lambda^H_\theta\right)^2\left(\lambda^0_{\mathrm{el}(z)}\lambda^N_z\right)^2}\right) \\ & + \lambda^0_{\mathrm{col}(\theta)}\lambda_{\mathrm{rem}(\theta)}\lambda^H_\theta \sum_{j=1}^{4}\gamma^{(j)H}\varphi^{(j)H}_{\mathrm{col}}\left\{\mathrm{c}^{(j)\mathrm{c}}_1\left(\left(\lambda^{(j)H}_{\mathrm{col}}\right)^2 - 1\right)\right. \\ & \left.\times \exp\left[\mathrm{c}^{(j)\mathrm{c}}_2\left(\left(\lambda^{(j)H}_{\mathrm{col}}\right)^2 - 1\right)^2\right]\right\}\sin^2\beta^{(j)N}_0 \\ & + \sum_{j=1}^{4}\mathrm{c}_{\mathrm{col}}\Delta\lambda^{(j)H}_r \int_0^{\hat{\alpha}^{(j)H}_{(i)}} \varphi^{(j)H}_{\mathrm{col}(i)}E^{(j)H}_{\mathrm{col}(i)}\left(\frac{\lambda^H_\theta}{\lambda^{(j)H}_{r(i)}}\right)^2 \sin^2\beta^{(j)H}d\alpha^{(j)H}_{(i)}\end{aligned}$$

and

$$\begin{aligned}\sigma^H_z = {} & 2\varphi^H_{\mathrm{el}}\mathrm{c}_{\mathrm{el}}\left(\left(\lambda^0_{\mathrm{el}(z)}\lambda^N_z\right)^2 - \frac{1}{\left(\lambda^0_{\mathrm{el}(\theta)}\lambda_{\mathrm{rem}(\theta)}\lambda^H_\theta\right)^2\left(\lambda^0_{\mathrm{el}(z)}\lambda^N_z\right)^2}\right) \\ & + \lambda^0_{\mathrm{col}(z)}\lambda^N_z \sum_{j=1}^{4}\gamma^{(j)H}\varphi^{(j)H}_{\mathrm{col}}\left\{\mathrm{c}^{(j)\mathrm{c}}_1\left(\left(\lambda^{(j)H}_{\mathrm{col}}\right)^2 - 1\right)\right. \\ & \left.\times \exp\left[\mathrm{c}^{(j)\mathrm{c}}_2\left(\left(\lambda^{(j)H}_{\mathrm{col}}\right)^2 - 1\right)^2\right]\right\}\cos^2\beta^{(j)N}_0 \\ & + \sum_{j=1}^{4}\mathrm{c}_{\mathrm{col}}\Delta\lambda^{(j)H}_r \int_0^{\hat{\alpha}^{(j)H}_{(i)}} \varphi^{(j)H}_{\mathrm{col}(i)}E^{(j)H}_{\mathrm{col}(i)}\left(\frac{\lambda^N_z}{\lambda_{\mathrm{rem(z)}}\lambda^{(j)H}_{r(i)}}\right)^2 \\ & \times \cos^2\beta^{(j)H}d\alpha^{(j)H}_{(i)}\end{aligned} \tag{12}$$

where $\lambda^{(j)H}_{r(i)} = \lambda^{(j)H}_{r(\min)} + \alpha^{(j)H}_{(i)}\Delta\lambda^{(j)H}_r$; $\Delta\lambda^{(j)H}_r = \lambda^{(j)H}_{r(\max)} - \lambda^{(j)H}_{r(\min)}$

$$\hat{\alpha}^{(j)H}_{(i)} = \begin{cases} 0 & \text{if } \lambda^{(j)H} < \lambda^{(j)H}_{r(\min)} \\ \dfrac{\lambda^{(j)H} - \lambda^{(j)H}_{r(\min)}}{\Delta\lambda^{(j)H}_r} & \text{if } \lambda^{(j)H}_{r(\min)} < \lambda^{(j)H} < \lambda^{(j)H}_{r(\max)} \\ 1 & \text{if } \lambda^{(j)H} > \lambda^{(j)H}_{r(\max)} \end{cases}$$

$$\gamma^{(j)H} = \begin{cases} 1 & \text{if } \lambda^{(j)H}_{\mathrm{col}} < 1 \\ 0 & \text{if } \lambda^{(j)H}_{\mathrm{col}} \geq 1 \end{cases}$$

$\lambda^{(j)H}_{\mathrm{col}} = \sqrt{(\lambda^0_{\mathrm{col}(\theta)}\lambda_{\mathrm{rem}(\theta)}\lambda^H_\theta)^2\sin^2\beta^{(j)N}_0 + (\lambda^0_{\mathrm{col}(z)}\lambda^N_z)^2\cos^2\beta^{(j)N}_0}$ and $\lambda^{(j)H} = \sqrt{(\lambda^H_\theta)^2\sin^2\beta^{(j)H} + (\lambda^H_z)^2\cos^2\beta^{(j)H}}$ are the stretches of a linear element oriented along the jth family of the collagen with respect to collagen and tissue natural state, respectively; $\lambda^{(j)H}_{\mathrm{col}(i)} = \lambda^{(j)H}/\lambda^{(j)H}_{r(i)}$ and $E^{(j)H}_{\mathrm{col}(i)} = \frac{1}{2}\left(\left(\lambda^{(j)H}_{\mathrm{col}(i)}\right)^2 - 1\right)$ are the stretch and the corresponding Green strain experienced by collagen fibers when they are straightened and stretched.

Following the global growth approach, we seek outcomes of remodeling in κ^H_0 (Fig. 1) that comply with requirements for restoration of arterial homeostasis under load as it exists in the normotensive artery. It has been experimentally established that provided blood flow remains unchanged, adaptive hypertension-induced remodeling restores the normotensive level of flow-induced shear stress at the endothelium (cf., Refs. [3] and [38–40]), which implies restoration of the deformed inner radius $r^H_i = r^N_i$. With an account for Eq. (6)

$$\lambda^H_\theta\left(R^H_i + \frac{H^H}{2}\right) - \frac{H^H}{2\lambda^H_\theta\lambda^H_z} - r^N_i = 0 \tag{13}$$

The requirement for restoration of the mean circumferential stress $\sigma^H_\theta = \sigma^N_\theta$ yields

$$\begin{aligned}& 2\varphi^H_{\mathrm{el}}\mathrm{c}_{\mathrm{el}}\left(\left(\lambda^0_{\mathrm{el}(\theta)}\lambda_{\mathrm{rem}(\theta)}\lambda^H_\theta\right)^2 - \frac{1}{\left(\lambda^0_{\mathrm{el}(\theta)}\lambda_{\mathrm{rem}(\theta)}\lambda^H_\theta\right)^2\left(\lambda^0_{\mathrm{el}(z)}\lambda^N_z\right)^2}\right) \\ & + \lambda^0_{\mathrm{el}(\theta)}\lambda_{\mathrm{rem}(\theta)}\lambda^H_\theta \sum_{j=1}^{4}\gamma^{(j)H}\varphi^{(j)H}_{\mathrm{col}}\left\{\mathrm{c}^{(j)\mathrm{c}}_1\left(\left(\lambda^{(j)H}_{\mathrm{col}}\right)^2 - 1\right)\right. \\ & \left.\times \exp\left[\mathrm{c}^{(j)\mathrm{c}}_2\left(\left(\lambda^{(j)H}_{\mathrm{col}}\right)^2 - 1\right)^2\right]\right\}\sin^2\beta^{(j)N}_0 \\ & + \sum_{j=1}^{4}\mathrm{c}_{\mathrm{col}}\Delta\lambda^{(j)H}_r \int_0^{\hat{\alpha}^{(j)H}_{(i)}} \varphi^{(j)H}_{\mathrm{col}(i)}E^{(j)H}_{\mathrm{col}(i)}\left(\frac{\lambda^H_\theta}{\lambda^{(j)H}_{r(i)}}\right)^2 \sin^2\beta^{(j)H}d\alpha^{(j)H}_{(i)} \\ & - \sigma^N_\theta = 0\end{aligned} \tag{14}$$

It follows from the free-body diagram of the inflated artery that $\sigma^H_\theta = P^H r^H_i/h^H$. Using the corresponding equation for normotensive artery given in Sec. 2.1, and the conditions $r^H_i = r^N_i$ and $\sigma^H_\theta = \sigma^N_\theta$, the equilibrium equation of hypertensive artery yields

$$\frac{H^H}{\lambda^H_\theta\lambda^H_z} - \frac{H^N}{\lambda^N_\theta\lambda^N_z}\frac{P^H}{P^N} = 0 \tag{15}$$

In agreement with experimental findings in Ref. [41], we did not impose a condition for restoration of the normotensive value of the axial stress.

In summary, the direct determination of the final outputs of remodeling is reduced to solving a system of algebraic and

transcendental equations that describe the change in mass fractions due to remodeling (Eqs. (7)–(9)), restoration of self-equilibration of the partial stresses borne by elastin and collagen in circumferential and axial directions (Eq. (10)), relations between the collagen family specific mass fractions and corresponding model parameters (Eq. (11)), restoration of the deformed inner radius (Eq. (13)), restoration of the target circumferential stress (Eq. (14)), and equilibrium of the hypertensive artery (Eq. (15)). Depending on the number of considered collagen fiber families, in total, the systems consist of eight (or nine or ten) equations. The system includes eight (or nine or ten) unknown model parameters as follows: geometrical parameters, R_i^H and H^H, constituents mass fractions φ_{el}^H and $\varphi_{\text{col}}^{(j)H}$, deformation parameters $\lambda_{\text{rem}(\theta)}$, $\lambda_{\text{rem}(z)}$, and λ_θ^H, and one (or two or three) mass fraction-related parameters $k_{\text{col}}^{(j)H}$. The only free parameter is the elevated pressure P^H that explicitly appears in Eqs. (8) and (15). Though the system is highly nonlinear, it is solvable using commercially available programs.

3 Illustrative Simulations

To illustrate the descriptive and predictive capability of the proposed model, we used a published constitutive model for a primary porcine renal artery [29]. The selected analytical form of the mass fraction intensity function is the so-called bell-shaped function

$$\varphi_{\text{col}(i)}^{(j)} = \left\{ k_{\text{col}}^{(j)M} \left[\left(\lambda_{r(\min)}^{(j)M} - \lambda_{r(i)}^{(j)} \right) \left(\lambda_{r(i)}^{(j)} - \lambda_{r(\max)}^{(j)M} \right) \right] \right\}^{a^M}, \quad \lambda_{r(i)}^{(j)} \in \left(\lambda_{r(\min)}^{(j)M}, \lambda_{r(\max)}^{(j)M} \right) \tag{16}$$

where a^M and $k_{\text{col}}^{(j)M}$ are fiber-specific structural parameters; $M = N$ or H for normotensive and hypertensive artery, respectively.

The vessel under pressure of 13.33 kPa (100 mmHg) and in situ axial stretch λ^N is considered as a normotensive artery. The values of all input geometrical, material, and mechanical parameters are taken from Ref. [29] and given in Table 1. The normotensive artery undergoes a finite deformation characterized by a mean circumferential stretch $\lambda_\theta^N = 1.621$ and a corresponding mean circumferential stress $\sigma_\theta^N = 132.88$ kPa. We consider the artery to be kept at constant length and subjected to a sustained hypertensive pressure. There is a lack of experimental data that allow identification of Eq. (8), which specify the relations between an increase in elastin and collagen mass fractions and applied hypertensive pressure in case 2. For illustrative purposes, we selected the simplest linear dependence as follows:

$$\varphi_{\text{el}}^H = \left[1 + \mu_{\text{el}} \left(\frac{P^H}{P^N} - 1 \right) \right] \varphi_{\text{el}}^N, \quad \varphi_{\text{col}}^H = \left[1 + \mu_{\text{col}} \left(\frac{P^H}{P^N} - 1 \right) \right] \varphi_{\text{col}}^N \tag{17}$$

with $\mu_{\text{el}} = 0.10$ and $\mu_{\text{col}} = 0.35$.

To evaluate the effects of the modulated prestretch of elastin and collagen on remodeling outputs, we compare the results from case 1 with the results from a "fictitious scenario" (case 1_{fict}) in which remodeling alters the wall composition in an identical manner but does not affect the tissue natural configuration. In this case, the prestretch of elastin and the structural organization of collagen fibers remain unchanged. The governing system of equations follows from the system for case 1 after setting $\lambda_{\text{rem}(\theta)} = \lambda_{\text{rem}(z)} = 1$, and neglecting Eq. (10).

The commercially available numerical solver Maple™ 12 (Maplesoft™, Waterloo, ON, Canada) was used to solve the system of corresponding governing equations for each of the four cases, with consideration of ten values of hypertensive pressure over the interval [13.33, 26.67] kPa. The calculated ratio between deformed mean radius and wall thickness for both the normotensive and hypertensive arteries is bigger than 5.5, which justifies the 2D membrane approach. Figures 2–9 illustrate the results obtained for the hypertension-induced changes in arterial mass, constituent mass fractions, mechanical properties of the tissue, collagen fibers prestretch, collagen mass fraction distribution, collagen fiber engagement in load bearing, tissue stretch, ZSS geometry, and arterial response. Finally, the model predicts that remodeling induces an insignificant (less than 0.2%) change in fiber angle (results not shown).

Table 1 Model parameters (taken from Ref. [29])

Parameter	Symbol	Value
Initial outer radius	R_o^N	2.24 mm
Initial thickness	H^N	0.81 mm
Axial stretch in vivo	λ_z^N	1.23
Elastin mass fraction	φ_{el}^N	0.252
Total collagen mass fraction of a helical fiber	$\varphi_{\text{col}}^{(3,4)N}$	0.182
Fiber orientation angle in the tissue ZSS	$\beta^{(3,4)N}$	∓ 49.67 deg
Fiber orientation angle in the collagen ZSS	$\beta_0^{(3,4)N}$	∓55.04 deg
Minimal recruitment stretch	$\lambda_{r(\min)}^{(3,4)N}$	1.349
Maximal recruitment stretch	$\lambda_{r(\max)}^{(3,4)N}$	1.752
Bell shaped function parameter	a^N	3.81
Bell shaped function parameter	$k^{(3,4)N}$	30.732
Collagen circumferential prestretch	$\lambda_{\text{col}(\theta)}^0$	0.700
Collagen longitudinal prestretch	$\lambda_{\text{col}(z)}^0$	0.850
Elastin circumferential prestretch	$\lambda_{\text{el}(\theta)}^0$	1.102
Elastin longitudinal prestretch	$\lambda_{\text{el}(z)}^0$	1.040
Elastin material parameter	c_{el}	33.82 kPa
Collagen material parameter (compression)	$c_1^{(3,4)c}$	0.430 MPa
Collagen material parameter (compression)	$c_2^{(3,4)c}$	7.10
Collagen material parameter (tension)	c_{col}	200 MPa

4 Discussion

4.1 Novelty. The major novelty of the proposed model is the predictive result that if remodeling causes disproportional changes in elastin and collagen mass fractions, as typically observed, it causes a change in the prestretches of elastin and collagen and therefore stress interaction between them. This leads to a

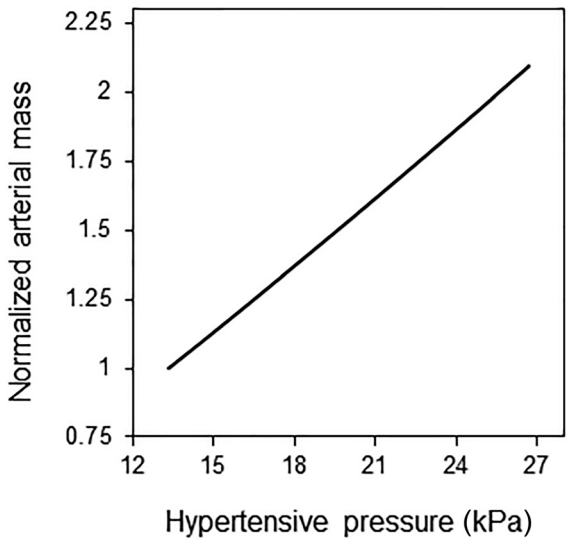

Fig. 2 Normalized arterial mass versus hypertensive pressure

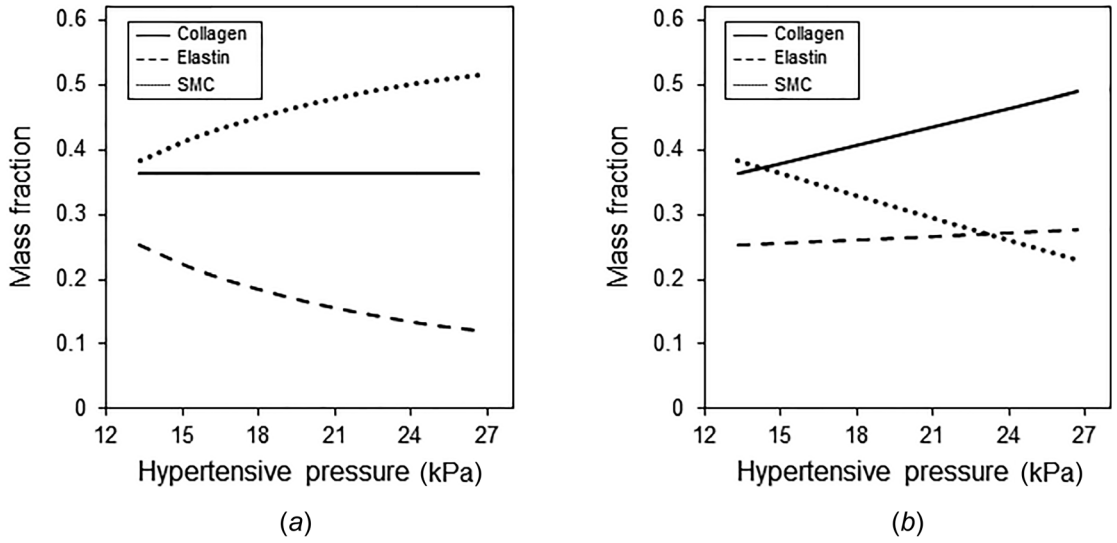

Fig. 3 Constituent mass fractions versus hypertensive pressure for (*a*) cases 1 and 1_{fict} (curves overlap) and (*b*) case 2

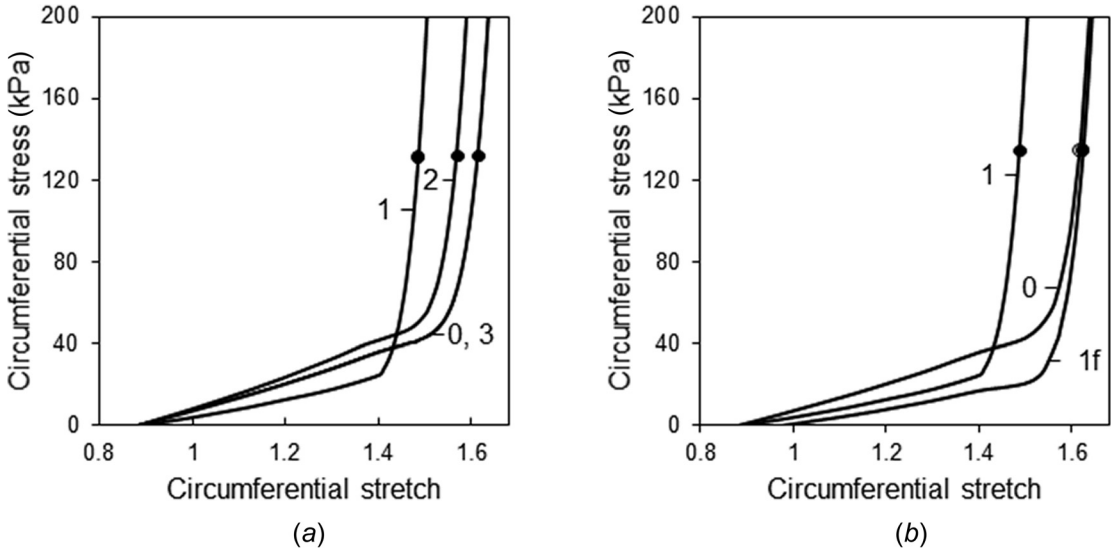

Fig. 4 Mean circumferential stress versus mean circumferential stretch. Case groupings highlight the (*a*) effects of tissue composition and the (*b*) individual effect of collagen network reorganization. Curve 0 refers to the normotensive artery; curves 1, 1f, 2, and 3 refer to the artery remodeled under sustained hypertensive pressure of 26.67 kPa in cases 1, 1_{fict}, 2, and 3, respectively. The (○) and (●) symbols denote an inflation pressure of 13.33 kPa and 26.67 kPa for the normotensive and hypertensive arteries, respectively.

reorganization of the collagen fiber network, which manifests as a fiber family specific reduction of fiber undulation and a change in direction of the helically oriented fibers in the tissue natural state. These changes have a significant impact on the arterial geometry and tissue mechanical properties after complete adaptive remodeling to elevated blood pressure.

4.2 Descriptive and Predictive Results. Having imposed restoration of deformed inner diameter and mean circumferential wall stress, the choice of any constitutive model can describe the deformed configuration and the amount of increased mass in the hypertensive artery because of the uniqueness of the state that restores mechanical homeostasis. The choice of an appropriate structure-based constitutive model and specification of remodeling-induced modulation of the amount of wall structural constituents, however, affects the new mass spatial distribution and tissue structural reorganization. The best approach to evaluate the predictive capacity of the proposed model is using known model parameters determined for a specific artery and a set of morphological, histological, and mechanical data of the normotensive vessel, as well as the analogous data of the remodeled hypertensive artery for different levels of elevated pressure. However, neither the model parameters nor corresponding experimental data relevant to a specific type artery are available. Therefore, we qualitatively evaluate the descriptive and predictive capabilities of the model on the basis of results taken from published data.

The existence of a unique solution of the system of transcendental governing equations verifies the potential of the proposed model to describe the adaptive remodeling response to sustained hypertension. In line with imposed conditions for restoration of the baseline value of the deformed inner diameter, increase in deformed wall thickness proportional to hypertensive pressure, and constant arterial length, the model predicts that the total mass

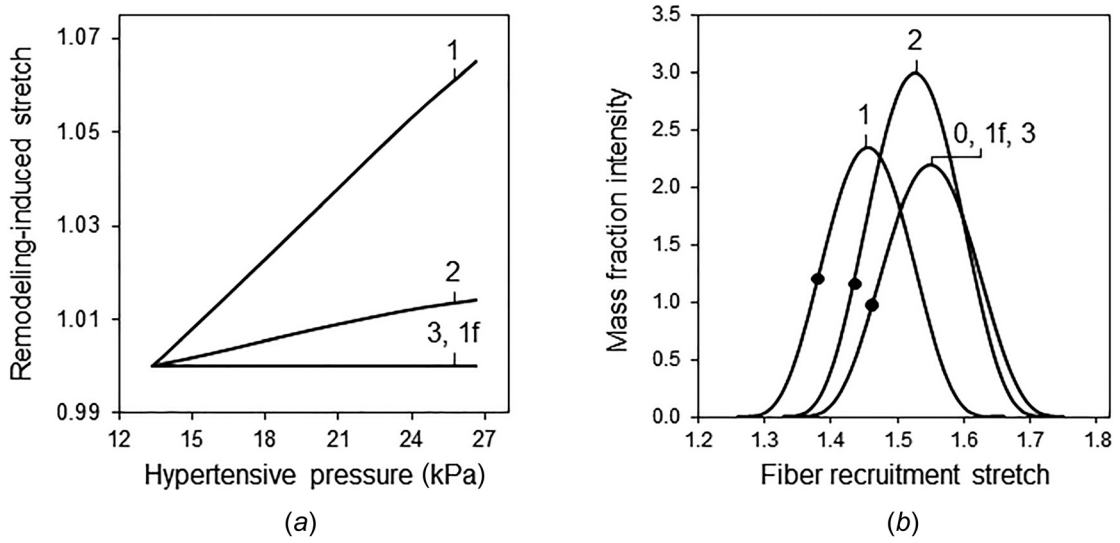

Fig. 5 Effects of remodeling on collagen fibers prestretch and mass fraction distribution. (*a*) Remodeling-induced stretch along the collagen fibers in the tissue ZSS versus hypertensive pressure. Curves 1, 1f, 2, and 3 refer to cases 1, 1_{fict}, 2, and 3, respectively. (*b*) Mass fraction intensity versus fiber recruitment stretch. Curve 0 refers to the normotensive artery; curves 1, 1f, 2, and 3 refer to the artery remodeled under sustained hypertensive pressure of 26.67 kPa in cases 1, 1_{fict}, 2, and 3, respectively. The (○) and (●) symbols denote an inflation pressure of 13.33 kPa and 26.67 kPa for the normotensive and hypertensive arteries, respectively.

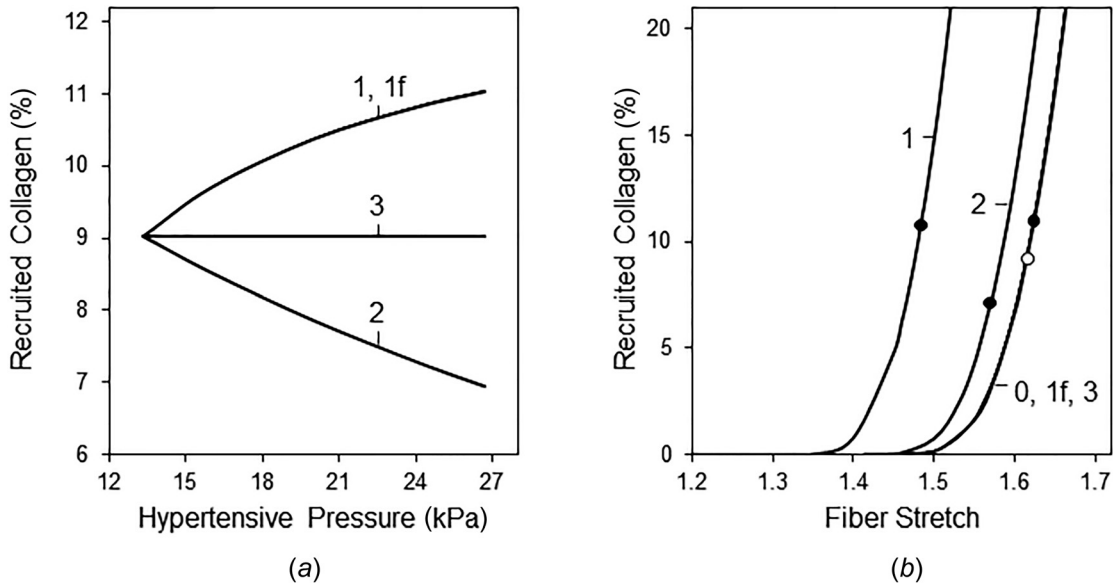

Fig. 6 Effects of remodeling on collagen fiber engagement. (*a*) Percentage of recruited collagen with respect to the total collagen versus hypertensive pressure. Curves 1, 1f, 2, and 3 refer to cases 1, 1_{fict}, 2, and 3, respectively. (*b*) Percentage of recruited collagen with respect to the total collagen versus fiber stretch. Curve 0 refers to the normotensive artery; curves 1, 1f, 2, and 3 refer to the artery remodeled under sustained hypertensive pressure of 26.67 kPa in cases 1, 1_{fict}, 2, and 3, respectively. The (○) and (●) symbols denote an inflation pressure of 13.33 kPa and 26.67 kPa for the normotensive and hypertensive arteries, respectively.

of the hypertensive artery does not depend on the adopted constitutive model and arterial mass increases virtually linearly with respect to the magnitude of the hypertensive pressure (Fig. 2). The factors and underlying processes that govern the synthetic activity, hypertrophy, and hyperplasia of SMCs, which ultimately result in a specific mass distribution among tissue constituents, are not completely known. The age of animals and chosen experimental model of sustained hypertension are plausible candidates. To simulate probable remodeling scenarios, we considered several typical cases prescribing the new mass distribution based on experimental findings reported in the literature as explained in Sec. 2. Excluding the trivial case 3 when the wall composition is not affected by remodeling, the dependence of wall composition on the magnitude of the hypertensive pressure is illustrated in Fig. 3. As prescribed by Eqs. (7) and (17), the mass fraction of elastin monotonically decreases with hypertensive pressure and collagen mass fraction remains unchanged in cases 1 and 1_{fict}, while both mass fractions monotonically increase with hypertensive pressure in case 2. It should be noted that in case 2, the calculated decrease in SMC mass fraction that results from the imposed increase in mass fraction of elastin and collagen does not imply that remodeling suppresses SMC hypotrophy and proliferation.

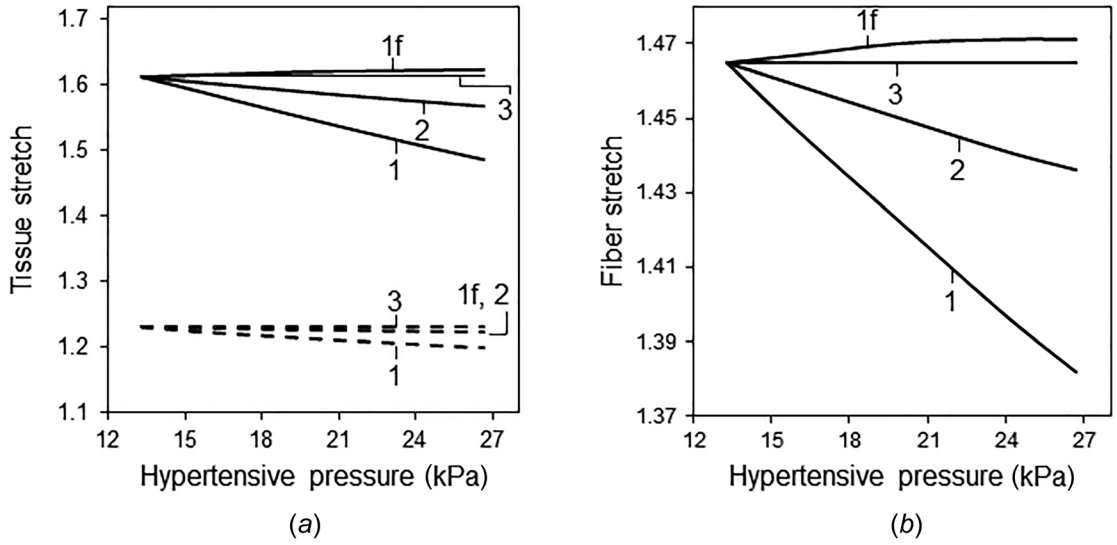

Fig. 7 Effects of remodeling on tissue stretch. (*a*) Circumferential stretch (continuous curves) and axial stretch (dashed curves) versus hypertensive pressure. (*b*) Stretch along collagen fibers versus hypertensive pressure. Curves 1, 1f, 2, and 3 refer to cases 1, 1_{fict}, 2, and 3, respectively.

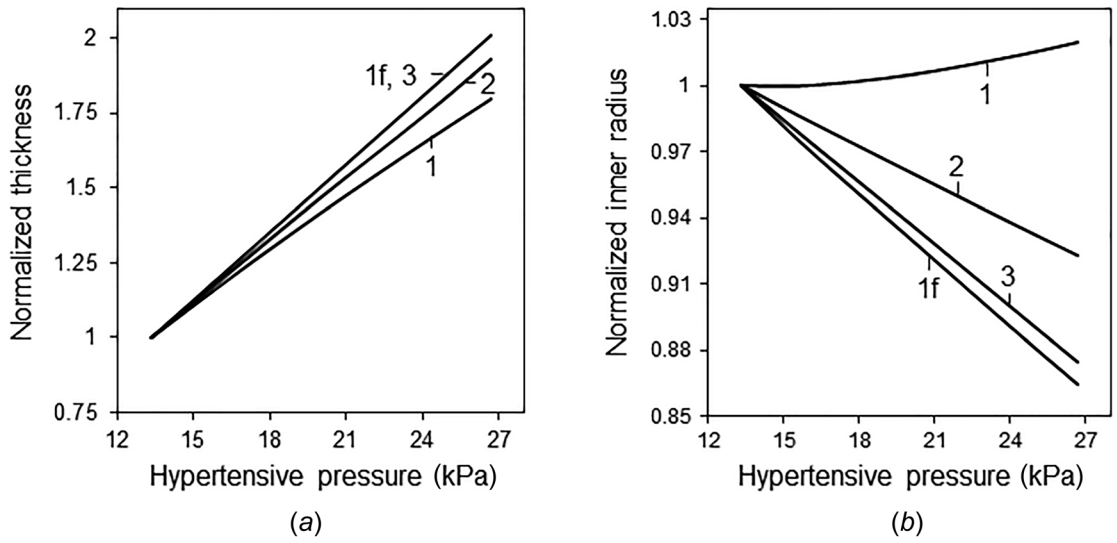

Fig. 8 (*a*) Normalized thickness versus hypertensive pressure. (*b*) Normalized inner radius versus hypertensive pressure. Curves 1, 1f, 2, and 3 refer to cases 1, 1_{fict}, 2, and 3, respectively.

Accounting for the fact that the total arterial mass increases with pressure (Fig. 2), the calculation of the amount of smooth muscle in the hypertensive artery remodeled under sustained hypertensive pressure of 26.67 kPa (200 mm Hg) is still 26% higher than the amount in the normotensive vessel.

One of the major predictive results of the proposed model is the hypertension-induced alteration of stress–stretch relations of arterial tissue. To evaluate the effects of remodeling on arterial tissue mechanical properties, we compared the circumferential stress–stretch responses of normotensive artery and hypertensive artery subjected to sustained pressure of 26.67 kPa (Fig. 4). Assuming no change in inherent mechanical properties of elastin and collagen, in the trivial case when constituent mass fractions are not affected by remodeling (case 3), the normotensive and the remodeled hypertensive artery exhibit an identical stress–stretch response regardless of the value of the hypertensive pressure (Fig. 4(*a*)). However, remodeling-induced change in elastin and collagen mass fractions modulates the constitutive relations via two different pathways. First, considering the tissue as a constrained mixture, mechanical properties are affected by the change in the elastin and collagen mass fractions that govern the individual contribution of constituents to load-bearing (cases 1, 1_{fict}, and 2). Second, because the ratio of elastin to collagen mass fraction of the hypertensive artery differs from the value of the normotensive artery, remodeling causes a change in prestretch of extended elastin and compressed collagen (cases 1 and 2).

Effects of remodeling on the mechanical properties of the hypertensive artery can be evaluated in two manners. The circumferential stretch needed to produce a certain value of the circumferential stress keeping the axial stretch fixed is a measure of global tissue stiffness. On the other hand, the slope of the stress–stretch curve at a certain stretch value is a measure of the local material stiffness and is related to the incremental modulus of the tissue. Over the elastin-dominated range of low tissue stretches (below 1.4), the stress response is governed by the mass fraction of elastin, its prestretch in the tissue natural state, and the stress borne by collagen fibers when they are compressed. At least in the cases under consideration, a change in elastin mass fraction

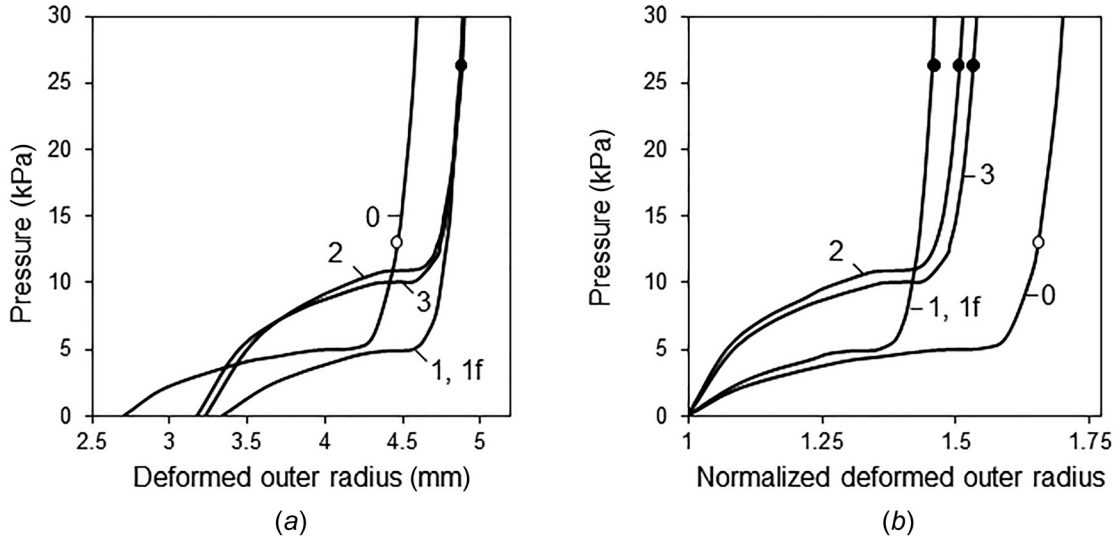

Fig. 9 Effects of remodeling on arterial response. (*a*) Deformed outer radius versus arterial pressure. (*b*) Normalized deformed outer radius versus arterial pressure (distension ratio curve). Curve 0 refers to the normotensive artery; curves 1, 1f, 2, and 3 refer to the artery remodeled under sustained hypertensive pressure of 26.67 kPa in cases 1, 1_{fict}, 2, and 3, respectively. The (○) and (●) symbols denote an inflation pressure of 13.33 kPa and 26.67 kPa for the normotensive and hypertensive arteries, respectively.

has the predominate effect and its decrease/increase causes a decrease/increase in both the global and local material stiffness compared to the normotensive artery (Fig. 4(*a*)). This conclusion is supported by the comparison between stress–stretch relations in cases 1 and 1_{fict} in which the changes in composition are identical, but in case 1_{fict}, the effects of remodeling on the tissue natural state are abolished. While due account of remodeling-induced changes in the tissue natural state increases the stress response over the elastin-dominated stretches, when compared at equivalent stretch, the tissue of hypertensive artery is softer than the tissue of the normotensive vessel (Fig. 4(*b*)).

At higher stretches, over the collagen-dominated stretch region, the tissue of the hypertensive artery in cases 1 and 2 is stiffer compared to the normotensive artery (Fig. 4(*a*)). The response is governed by the change in collagen mass fraction (case 2 only), structural reorganization of collagen, the percentage of collagen fibers involved in load-bearing, and the contribution of elastin. Opposite to the response over the elastin-dominated region of stretches, the altered stress response is governed mainly by the effects of remodeling on the manner by which collagen fibers are engaged in load-bearing. Figure 5(*a*) illustrates the dependence of remodeling-induced stretch along the fibers in the tissue natural state on the value of hypertension for considered cases of mass distribution. Accordingly, remodeling modifies the collagen mass fraction intensity function (Fig. 5(*b*)) and insignificantly the orientation of the helical fibers. Depending on the extent to which remodeling affects the ratio between elastin and collagen mass fraction (more in case 1 than in case 2, Fig. 3), the onset of collagen fiber engagement occurs at a lower tissue stretch, over a narrower range of stretches, and at an increased rate (Fig. 5(*b*)), with the net result of increased tissue stiffness in the hypertensive artery. Obviously, as a consequence of remodeling the model predicts that collagen fibers in an adapted hypertensive artery are less undulated in the tissue natural state compared to the normotensive artery, which agrees with the histological observations in Ref. [42]. As for the amount of collagen fibers engaged in load-bearing, Fig. 6 illustrates two typical predictions of the proposed model. The percentage of the mass fraction of "working" collagen fibers in the remodeled artery does not correlate with the total collagen mass fraction resulting from remodeling. When the total collagen mass fraction remains unchanged (case 1), the percentage of engaged collagen fibers monotonically increases with hypertensive pressure; when the total collagen mass fraction increases (case 2), the percentage of engaged collagen fibers decreases with hypertensive pressure (Fig. 6(*a*)). This difference is due to the fact that at given hypertensive pressure the percentage of the mass fraction of "working" collagen fibers is a net effect of changes in total arterial mass (Fig. 2), collagen mass fraction (Fig. 3), and the mass fraction intensity function (Fig. 5(*b*)). On the other hand, as expected, for a given remodeled artery, the percentage of the engaged collagen mass fraction increases with an increase in fiber stretch (Fig. 6(*b*)). Finally, the relatively low values of collagen fiber engagement in normotensive and hypertensive arteries agree with results of previous studies [29,43]. As discussed in Ref. [29], these values might result from overestimation of the accepted value of the collagen fiber modulus and need experimental verification.

The leading role of collagen reorganization on tissue stiffening is supported by the comparison of model predictions in cases 1 and 1_{fict}. In both the cases, the percentage of recruited collagen fibers is equal (Fig. 6(*a*)). If the stress interaction between elastin and collagen is neglected, the tissue of "fictitious" hypertensive artery is softer than the tissue of normotensive artery (Fig. 4(*b*)) and the stress response in the collagen-dominated stretch region is similar to that of the normotensive artery. Therefore increased global material stiffness of hypertensive arteries is due mainly to altered elastin-collagen stress interaction that makes the engagement of collagen fibers occur at lower stretch levels. At the target circumferential stress ($\sigma_\theta^N = 132.88$ kPa), the local material stiffness is governed by the value of the corresponding circumferential stretch and amount of collagen involved in load-bearing. Model-predicted similarity between the slope of hypertensive and normotensive arteries (Fig. 4) could not be considered as a general tendency but rather as a result of abrupt engagement of collagen over a narrow range of fiber stretch, which is predetermined by the selected bell-shaped mass fraction function and high value of the collagen material parameter (Table 1).

The effects of hypertension-induced remodeling on the stress–stretch relation are similar to the theoretical predictions for the stress response caused by a functional elastin degradation of renal artery in Ref. [29]. In both scenarios, a reduction of elastin mass fraction modulates the initial prestretch of elastin and collagen in the new tissue ZSS. However, the cause of diminished elastin mass fraction is different. In the case of hypertension-induced remodeling, this is due to the increase in the total arterial mass accompanied by no change (case 1) or even disproportionate

increases (case 2) in elastin mass, while elastin degradation reduces the elastin mass engaged in load-bearing but the total arterial mass remains unchanged.

The model predicts that hypertension causes an insignificant decrease in the longitudinal stretch in the deformed state of the remodeled artery (Fig. 7(*a*)), which is qualitatively supported by experimental observations in Refs. [44] and [45] that the in vivo axial strain was decreased by hypertension. In line with material stiffening in the circumferential direction, the circumferential stretch and the stretch in the direction of fibers gradually decrease with the increase in hypertensive pressure (cases 1 and 2 in Fig. 7). Again, the response is governed mainly by the remodeling-induced stress interaction between elastin and collagen. This conclusion is in concert with the model predictions for increased remodeling-induced stretch along collagen fibers (Fig. 5(*a*)), which lowers the minimal recruitment stretch in the hypertensive artery (Fig. 5(*b*)). If the stress interaction is neglected (case 1_{fict}), the stretches are very close to the values in case 3 in which remodeling does change tissue composition. A small discrepancy between the cases is due to the fact that case 1_{fict} still accounts for the decrease in elastin mass fraction and slightly higher stretch is needed to restore the target circumferential stress. In the case of no alteration in stress interaction between elastin and collagen due to preserved tissue composition (case 3), the constant fiber stretch at any hypertensive pressure (Fig. 7(*b*)), no remodeling-induced fiber stretch (Fig. 5(*a*)), and constant mode of collagen mass fraction intensity function (Fig. 5(*b*)) are logical consequences.

The decrease in stretch along fibers in the deformed arterial configuration suggests some plausible speculations for the causal link between this output of hypertension-induced remodeling and the reduced waviness of collagen fibers. Remodeling occurs simultaneously with continuous collagen turnover that maintains the collagen prestretch and collagen network organization. New mass is added in the deformed configuration, while the effects of collagen turnover, evaluated in terms of parameters that describe the fiber waviness, are observable in the natural arterial state. It seems reasonable to assume that the restoration of the local mechanical environment of SMCs leads to restoration of the normal mode of collagen fiber synthesis, and more specifically the value of the deposition stretch at which new fibers are laid down and integrated in the tissue under loads. The deposition stretch of collagen then seems to be a target parameter rather than a descriptor of the remodeling-induced change in the collagen stress response. If a constituent-specific deposition stretch is defined to be the stretch experienced by a structural constituent before being replaced by a new material, it is equal to the product of the corresponding prestretch and the tissue stretch in the deformed arterial state. Moreover, by virtue of Eq. (10), the prestretches of collagen and elastin are interrelated and the corresponding deposition stretches are also coupled. Because the model predicts that in hypertension, the collagen fibers are less compressed in the arterial natural state (the value of the effective collagen prestretch is closer to one), a constant deposition stretch requires a decrease in the circumferential stretch and stretch in the direction of fibers in the deformed state of the hypertensive artery as predicted by the model. Then new collagen fibers, which are laid down in the deformed arterial configuration, are less wavy in the tissue natural configuration.

Because stretches govern the mapping of the natural configuration to the deformed configuration, the ZSS dimensions of the remodeled hypertensive arteries are also case-specific. The results obtained show that the ZSS wall thickness increases with hypertensive pressure in all cases (Fig. 8(*a*)). This outcome was reported in many experimental investigations (cf., Refs. [3], and [40–42]) and was predicted by all published models for pressure-induced remodeling (cf., Refs. [4–10] and [15–17]). However, the relation between the ZSS inner radius and hypertensive pressure might trend differently depending on the manner by which remodeling affects the wall composition (Fig. 8). A common characteristic of cases 1 and 2 is that the hypertensive artery exhibits smaller ZSS inner radius/wall thickness ratio compared to case 3, despite the fact that the ratio between deformed thickness and deformed inner radius is equal for all cases. An interesting predictive result is that the ZSS inner radius is virtually constant for case 1, which is supported experimental findings for morphology and histology of the rat common carotid after induction of DOCA-salt hypertension reported in Ref. [33]. Therefore, the hypertension-induced chronic arterial response in case 1, evaluated in terms of geometrical dimensions in the ZSS, manifests as an adaptive outward hypertrophic remodeling according to the classification in Ref. [46]. Accounting for the fact that the value of the deformed inner radius of the remodeled hypertensive artery is also independent of the value of the hypertensive pressure, the constant value of the inner radius in the ZSS implies that remodeling restores also the baseline value of circumferential stretch experienced by the endothelial cells that modulate their gene expression [47]. Comparison between model predictions of cases 1 and 1_{fict} shows that ZSS geometry that manifests the true growth due to remodeling is strongly influenced by the stress interaction between elastin and collagen (Fig. 8(*b*)).

Altered ZSS geometry and mechanical properties of arterial tissue caused by the adaptive remodeling govern the mechanical response of the hypertensive artery. Predicted pressure–deformed outer radius curves show that regardless of constitutive relations of the arterial tissue, each hypertensive artery has equal outer deformed radius under the operating pressure of 26.67 kPa (Fig. 9(*a*)). This is an expected result due to the imposed kinematic condition for restoration of the deformed inner radius to a target value and the fact that deformed thickness does not depend on the mechanical properties of the wall material according to Eq. (15). An interesting result is a predicted virtual overlap of the curves corresponding to cases 1 and 1_{fict}, which means that remodeling-induced alteration of the initial prestretch of elastin and collagen does not meaningfully affect the mechanical response of artery. Recall that though mass fractions of constituents are equal, the mechanical properties and initial geometry in these cases are different. Thus, at least in the considered particular cases, while the structural reorganization of collagen fibers caused by remodeling significantly impacts material stiffness, the governing factor for the structural response is the composition of the arterial wall.

To eliminate the variation in initial arterial geometry on the experimental findings for effects of remodeling on the mechanical response, it is often illustrated as pressure–distension ratio curves using as a distension ratio the deformed outer radius normalized by the radius at zero pressure (Fig. 9(*b*)). The model predicts that at equivalent pressures the distension ratio of hypertensive arteries is smaller than the ratio of the normotensive artery, showing that remodeling increases the structural stiffness. In all considered cases, the slope of the pressure–distention ratio curve is higher than the slope of the normotensive artery, with a tendency for the difference to decrease at higher pressure when collagen is the dominant load-bearing constituent. These conclusions are in qualitative agreement with reported experimental data in Ref. [40]. As expected, the effect is more pronounced over the physiological pressure range in which the contribution of collagen to tissue mechanical properties is dominant. A comparison between the pressure–distension ratios curves in cases 1 and 1_{fict} again shows that they are virtually identical. Despite the fact that remodeling alters in a different manner the mechanical properties of the tissue and initial dimensions of the vessel, the identical wall composition, deformed inner diameter, and wall thickness under hypertensive pressure are sufficient to yield a virtually identical arterial response over the entire pressure range.

4.3 Limitations and Perspectives. To focus on the novelty of the model, namely the effects of stress interaction between elastin and collagen on remodeling outputs, we introduced several assumptions that significantly simplify the numerical calculations and interpretations of the model predictions. An artery is considered as a one-layered elastic membrane and contribution of smooth muscle to the mechanical response is neglected. Similar to all published models on pressure-induced remodeling, we

assumed that inherent mechanical properties of collagen fibers and elastin do not change. The manner of distribution of remodeling-induced increase in arterial mass among structural constituents was prescribed on the basis of some general speculation. It is well known that different experimental approaches to induce hypertension might yield contradictory experimental results, but our model does not address this issue.

Another group of limitations in our study refers to the performed illustrative simulations. As discussed in Sec. 3, all model parameters were taken from published data instead of determined from morphological, histological, and inflation–extension data of a single artery, though there are reliable methods for model parameter identification from histological assays, optical methods such as confocal and scanning electron microscopy, and morphological data after enzymatic degradation of elastin [29]. Similarly, selection of the deterministic bell-shaped function, Eq. (16), is based on heuristic consideration rather than on experimental findings. Therefore, the results obtained in our study underline the importance of accounting for the stress interaction between elastin and collagen, but remain at best mainly illustrative. There is a pressing need of more numerical simulations and parametric analyses for arteries from different locations and age groups.

Refinements of the proposed model might go in several directions. It is reasonable to generalize the model to three-dimensions, and to account for passive and active smooth muscle, anisotropic mechanical properties of elastin, distribution of collagen fibers around a primary orientation direction, and the difference between the medial and adventitial layers. Most likely, remodeling affects not only collagen network organization but also collagen fiber cross-linking [2]. Moreover, recent studies suggest that the clinical importance of model predictions would be increased by refinements which reflect factors such as inflammation that leads to maladaptive remodeling [20,21] and conditions on time variation of elevated pressure under which remodeling might be considered as a quasi-static process [28]. A vital task for adequate mathematical modeling is motivated selection of equations that describe the distribution of new mass among arterial wall constituents and between media and adventitia, which is expected to be specific for different modes of experimental hypertension as done in Refs. [22] and [23]. In line with the specifics of the adopted constitutive model [29], a critical point is the necessity of model-motivated experiments to identify layer-specific prestretches of elastin and collagen and mass distribution among fibers with identical orientation but different waviness in terms of mass fraction intensity functions of recruitment stretches.

5 Conclusion

In conclusion, we proposed a novel 2D mathematical model for obtaining predictive results of adaptive hypertension-induced remodeling of arteries. The model is based on a structure-based constitutive model of arterial tissue that explicitly considers the individual zero-stress configurations of elastin and collagen and their interactions in terms of the constituents' specific prestretches in the tissue natural state. The model is built in the framework of the global growth approach and aims at obtaining the zero-stress geometry, arterial wall composition, structural organization of collagen network, and mechanical response of the hypertensive artery when adaptive pressure-induced remodeling is completed. Better understanding the process and consequences of adaptive remodeling allows revealing the probable causes and modes of maladaptive arterial remodeling in response to hypertension, which manifests as the generation and progression of certain vascular disorders. Moreover, the model promotes better understanding of experimental and clinical data and motivates directions for future studies on arterial remodeling.

Funding Data

- National Science Foundation (NSF), BMMB-Biomech & Mechanobiology (Award No. 1760906; Funder ID: 10.13039/100000001).

References

[1] Thorn, S., 1997, "Arterial Structural Modifications in Hypertension. Effects of Treatment," Eur. Heart J., **18**(Suppl. E), pp. E2–E4.
[2] Humphrey, J. D., 2008, "Mechanisms of Arterial Remodeling in Hypertension: Coupled Roles of Wall Shear and Intramural Stress," Hypertension, **52**(2), pp. 195–200.
[3] Hayashi, K., and Naiki, T., 2009, "Adaptation and Remodeling of Vascular Wall; Biomechanical Response to Hypertension," J. Mech. Behav. Biomed. Mater., **2**(1), pp. 3–19.
[4] Taber, L. A., and Eggers, D. W., 1996, "Theoretical Study of Stress-Modulated Growth in the Aorta," J. Theor. Biol., **180**(4), pp. 343–357.
[5] Rachev, A., Stergiopulos, N., and Meister, J. J., 1996, "Theoretical Study of Dynamics of Arterial Wall Remodeling in Response to Changes in Blood Pressure," J. Biomech., **29**(5), pp. 635–642.
[6] Taber, L. A., 1998, "A Model for Aortic Growth Based on Fluid Shear and Fiber Stresses," ASME J. Biomech. Eng., **120**(3), pp. 348–354.
[7] Alford, P. W., Humphrey, J. D., and Taber, L. A., 2008, "Growth and Remodeling in a Thick-Walled Artery Model: Effects of Spatial Variations in Wall Constituents," Biomech. Model Mechanobiol., **7**(4), pp. 245–262.
[8] Raykin, J., Rachev, A. I., and Gleason, R. L., 2009, "A Phenomenological Model for Mechanically Mediated Growth, Remodeling, Damage, and Plasticity of Gel-Derived Tissue Engineered Blood Vessels," ASME J. Biomech. Eng., **131**(10), p. 101016.
[9] Rachev, A., and Gleason, R. L., Jr., 2011, "Theoretical Study on the Effects of Pressure-Induced Remodeling on Geometry and Mechanical Non-Homogeneity of Conduit Arteries," Biomech. Model Mechanobiol., **10**(1), pp. 79–93.
[10] Rachev, A., Stergiopulos, N., and Meister, J. J., 1998, "A Model for Geometric and Mechanical Adaptation of Arteries to Sustained Hypertension," ASME J. Biomech. Eng., **120**(1), pp. 9–17.
[11] Tsamis, A., Stergiopulos, N., and Rachev, A., 2009, "A Structure-Based Model of Arterial Remodeling in Response to Sustained Hypertension," ASME J Biomech. Eng., **131**(10), p. 101004.
[12] Fridez, P., Rachev, A., Meister, J. J., Hayashi, K., and Stergiopulos, N., 2001, "Model of Geometrical and Vascular Smooth Muscle Tone Adaptation of Carotid Artery Subjected to Step Change in Pressure," Am. J. Physiol.: Heart Circ. Physiol., **280**(6), pp. H2752–H2760.
[13] Rachev, A., Manoach, E., Berry, J., and Moore, J. E., Jr., 2000, "A Model of Stress-Induced Geometrical Remodeling of Vessel Segments Adjacent to Stents and Artery/Graft Anastomoses," J. Theor. Biol., **206**(3), pp. 429–443.
[14] Humphrey, J. D., and Rajagopal, K. R., 2002, "A Constrained Mixture Model for Growth and Remodeling of Soft Tissues," Math. Models Methods Appl. Sci., **12**(3), pp. 407–430.
[15] Gleason, R. L., and Humphrey, J. D., 2004, "A Mixture Model of Arterial Growth and Remodeling in Hypertension: Altered Muscle Tone and Tissue Turnover," J. Vasc. Res., **41**(4), pp. 352–363.
[16] Wan, W., Hansen, L., and Gleason, R. L., 2010, "A 3-D Constrained Mixture Model for Mechanically Mediated Vascular Growth and Remodeling," Biomech. Model. Mechanobiol., **9**(4), pp. 403–419.
[17] Karsaj, I., and Humphrey, J. D., 2012, "A Multilayered Wall Model of Arterial Growth and Remodeling," Mech. Mater., **44**, pp. 110–119.
[18] Valentın, A., Cardamone, L., Baek, S., and Humphrey, J. D., 2009, "Complementary Vasoactivity and Matrix Remodelling in Arterial Adaptations to Altered Flow and Pressure," J. R. Soc. Interface, **6**(32), pp. 293–306.
[19] Valentín, A., and Humphrey, J. D., 2009, "Evaluation of Fundamental Hypotheses Underlying Constrained Mixture Models of Arterial Growth and Remodelling," Philos. Trans. R. Soc., A, **367**(1902), pp. 3585–3606.
[20] Latorre, M., and Humphrey, J. D., 2018, "Modeling Mechano-Driven and Immuno-Mediated Aortic Maladaptation in Hypertension," Biomech. Model. Mechanobiol., **17**(5), pp. 1497–1511.
[21] Latorre, M., Bersi, M. R., and Humphrey, J. D., 2019, "Computational Modeling Predicts Immuno-Mechanical Mechanisms of Maladaptive Aortic Remodeling in Hypertension," Int. J. Eng. Sci., **141**, pp. 35–46.
[22] Bersi, M. R., Bellini, C., Wu, J., Montaniel, K. R. C., Harrison, D. G., and Humphrey, J. D., 2016, "Excessive Adventitial Remodeling Leads to Early Aortic Maladaptation in Angiotensin-Induced Hypertension," Hypertension, **67**(5), pp. 890–896.
[23] Bersi, M. R., Khosravi, R., Wujciak, A. J., Harrison, D. G., and Humphrey, J. D., 2017, "Differential Cell-Matrix Mechanoadaptations and Regional Propensities to Aortic Fibrosis, Aneurysm, or Dissection in Hypertension," J. R. Soc. Interface., **14**(136), p. 20170327.
[24] Valentın, A., Humphrey, J. D., and Holzapfel, G. A., 2011, "A Multi-Layered Computational Model of Coupled Elastin Degradation, Vasoactive Dysfunction, and Collagenous Stiffening in Aortic Aging," Ann. Biomed. Eng., **39**(7), pp. 2027–2045.
[25] Wilson, J. S., Baek, S., and Humphrey, J. D., 2012, "Importance of Initial Aortic Properties on the Evolving Regional Anisotropy, Stiffness and Wall Thickness of Human Abdominal Aortic Aneurysms," J. R. Soc. Interface., **9**(74), p. 2047.
[26] Rachev, A., 1997, "Theoretical Study of the Effect of Stress-Dependent Remodeling on Arterial Geometry Under Hypertensive Conditions," J. Biomech., **30**(8), pp. 819–827.
[27] Rachev, A., Taylor, W. R., and Vito, R. P., 2013, "Calculation of the Outcomes of Remodeling of Arteries Subjected to Sustained Hypertension Using a 3D Two-Layered Model," Ann. Biomed. Eng., **41**(7), pp. 1539–1553.
[28] Latorre, M., and Humphrey, J. D., 2018, "Critical Roles of Time-Scales in Soft Tissue Growth and Remodeling," APL Bioeng., **2**(2), p. 026108.
[29] Rachev, A., and Shazly, T., 2019, "A Structure-Based Constitutive Model of Arterial Tissue Considering Individual Natural Configurations of Elastin and Collagen," J. Mech. Behav. Biomed. Mater., **90**, pp. 61–72.

[30] Humphrey, J. D., 2001, *Cardiovascular Solid Mechanics*, Springer-Verlag, New York.
[31] Rachev, A., 2003, "Remodeling of Arteries in Response to Changes in Their Mechanical Environment," *Biomechanics of Soft Tissue in Cardiovascular Systems*, G. A. Holzapfel, and R. W. Ogden, eds., Springer-Verlag, Wien, Austria, pp. 221–271.
[32] Rezakhaniha, R., Agianniotis, A., Schrauwen, J. T., Griffa, A., Sage, D., Bouten, C. V., van de Vosse, F. N., Unser, M., and Stergiopulos, N., 2012, "Experimental Investigation of Collagen Waviness and Orientation in the Arterial Adventitia Using Confocal Laser Scanning Microscopy," Biomech. Model. Mechanobiol., **11**(3–4), pp. 461–473.
[33] Hayashi, K., and Shimizu, E., 2016, "Composition of Connective Tissues and Morphometry of Vascular Smooth Muscle in Arterial Wall of DOCA-Salt Hypertensive Rats—In Relation With Arterial Remodeling," J. Biomech., **49**(7), pp. 1225–1229.
[34] Wolinsky, H., 1971, "Effect of Hypertension and Its Reversal on the Thoracic Aorta of Male and Female Rats: Morphological and Chemical Studies," Circ. Res., **28**(6), pp. 622–637.
[35] Wolinsky, H., 1972, "Long-Term Effects of Hypertension on the Rat Aortic Wall and Their Relation to Concurrent Aging Changes: Morphological and Chemical Studies," Circ. Res., **30**(3), pp. 301–309.
[36] Fridez, P., Zulliger, M., Bobard, F., Montorzi, G., Miyazaki, H., Hayashi, K., and Stergiopulos, N., 2003, "Geometrical, Functional, and Histomorphometric Adaptation of Rat Carotid Artery in Induced Hypertension," J. Biomech., **36**(5), pp. 671–680.
[37] Brayden, J. E., Halpern, W., and Brann, L. R., 1983, "Biochemical and Mechanical Properties of Resistance Arteries From Normotensive and Hypertensive Rats," Hypertension, **5**(1), pp. 17–25.
[38] Fung, Y. C., and Liu, S. Q., 1989, "Change of Residual Strains in Arteries Due to Hypertrophy Caused by Aortic Constriction," Circ. Res., **65**(5), pp. 1340–1349.
[39] Liu, Q., and Fung, Y. C., 1989, "Relationship Between Hypertension, Hypertrophy and Opening Angle of Zero-Stress State of Arteries Following Aortic Constriction," ASME J. Biomech. Eng., **111**(4), pp. 325–335.
[40] Matsumoto, T., and Hayashi, K., 1994, "Mechanical and Dimensional Adaptation of Rat Aorta to Hypertension," ASME J. Biomech. Eng., **116**(3), pp. 278–283.
[41] Matsumoto, T., and Hayashi, K., 1996, "Response of Arterial Wall to Hypertension and Residual Stress," *Biomechanics—Functional Adaptation and Remodeling*, K. Hayashi, A. Kamiya, and K. Ono, eds., Springer-Verlag, Tokyo, Japan, pp. 93–119.
[42] Tsamis, A., Krawiec, J. T., and Vorp, D. A., 2013, "Elastin and Collagen Fiber Microstructure in the Human Aorta in Ageing and Disease: A Review," J. R. Soc. Interface, **10**(83), p. 20121004.
[43] Zulliger, M. A., Fridez, P., Hayashi, K., and Stergiopulos, N., 2004, "A Strain Energy Function for Arteries Accounting for Wall Composition and Structure," J. Biomech., **37**(7), pp. 989–1000.
[44] Wolinsky, H., 1970, "Response of the Aortic Media to Hypertension: Morphological and Chemical Studies," Circ. Res., **26**(4), pp. 507–522.
[45] Vaishnav, R. N., Vossoughi, J., Patel, D. J., Cothran, L. N., Coleman, B. R., and Ison-Franklin, E. L., 1990, "Effect of Hypertension on Elasticity and Geometry of Aortic Tissue From Dogs," ASME J. Biomech. Eng., **112**(1), pp. 70–74.
[46] Mulvany, M. J., Baumbach, G. L., Aalkjaer, C., Heagerty, A. M., Korsgaard, N., Schiffrin, E. L., and Heistad, D. D., 1996, "Vascular Remodeling," Hypertension, **28**(3), pp. 505–506.
[47] Xu, J., and Shi, G. P., 2014, "Vascular Wall Extracellular Matrix Proteins and Vascular Diseases," Biochim. Biophys. Acta, **1842**(11), pp. 2106–2119.